Self-Localized States in Photonic Topological Insulators

Yaakov Lumer, Yonatan Plotnik, Mikael C. Rechtsman, and Mordechai Segev

Physics Department and the Solid State Institute, Technion – Israel Institute of Technology, Haifa 32000, Israel

(Received 25 September 2013; published 12 December 2013)

We propose solitons in a photonic topological insulator: self-localized wave packets forming topological edge states residing in the bulk of a nonlinear photonic topological insulator. These self-forming entities exhibit, despite being in the bulk, the property of unidirectional transport, similar to the transport their linear counterparts display on the edge of a topological insulator. In the concrete case of a Floquet topological insulator, such a soliton forms when a wave packet induces, through nonlinearity, a defect region in a honeycomb lattice of helical optical waveguides, and at the same time the wave packet populates a continuously rotating outer (or inner) edge state of that region. The concept is universal and applicable to topological systems with nonlinear response or mean-field interactions.

DOI: 10.1103/PhysRevLett.111.243905 PACS numbers: 42.65.Jx, 42.65.Sf, 42.65.Tg

Topological insulators are a new state of matter [1–4] with the striking property of robust, scatter-free conduction on the edges in the two-dimensional case. Such scatter-free conduction manifests itself in the topological protection of the edge states, which arises from strong spin-orbit coupling and a fermionic property called ‘‘Kramer's degeneracy’’ [5]. Similar robust and scatter-free edge conduction can be achieved by applying a strong magnetic field, thus breaking time-reversal symmetry and giving rise to the quantum Hall effect [6]. In the past few years, there have been numerous propositions to realize topological insulation for electromagnetic waves [7–12]. Apart from many intriguing issues having to do with topological protection in photonic media, the study of photonic topological insulators can lead to advances in many related areas. For example, optical delay lines can be made more robust by topologically protected transport [10]. Likewise, the unidirectionality feature of topological insulators can offer novel designs for optical isolators [12]. In a different domain, the mathematical equivalence between the Schrödinger equation and the paraxial wave equation in photonics [13,14] opens up the possibility of exploring related novel phenomena such as topological Anderson insulators [15] and Floquet topological insulators [16–18], which are exceedingly difficult to study experimentally in solid state systems.

The bosonic nature of photons implies the necessity of a different mechanism to achieve topological protection. One path to achieve the goal of scatter-free propagation is similar to the quantum Hall effect, where a strong magnetic field is used to break time-reversal symmetry and hence eliminate backscattering. Indeed, this idea was suggested [7,19] and demonstrated experimentally [20] in gyro-optic photonic crystals, where the magnetic field induces topological protected edge states. However, magnetic effects are negligibly small at optical frequencies. Hence, a number of theoretical suggestions were made [8–12] for designing a field-free photonic medium with topologically protected transport. The first experimental demonstration of such a system was published recently [21], drawing on the idea of Floquet topological insulators, in which specifically designed modulation gives rise to topological protection [16,17,22,23]. That particular photonic topological insulator was implemented in ‘‘photonic graphene’’ [24], an array of waveguides arranged as a honeycomb lattice, where the modulation causing the topological protection was achieved by making the waveguides helical [21]. Another demonstration of topological edge states, in coupled resonator arrays, followed later [25], and similar attempts are currently under way in cold atoms systems.

This Letter deals with nonlinear effects in photonic topological insulators. Indeed, nonlinearity is a fundamental aspect of optics. It allows for light to control light via the nonlinear response, and enables a variety of important phenomena such as spatial solitons [26], modulation instability [27], frequency conversion and more. Furthermore, when the optical nonlinearity is of the Kerr type, there is a direct mathematical equivalence between nonlinear optics, described by the nonlinear Schrödinger equation and the mean-field description of interactions in Bose-Einstein condensates [13,14]. Therefore, studying nonlinear aspects of photonic topological insulators may also lead to advances in the understanding of topological phenomena in other physical realizations.

Here, we propose solitons in a photonic topological insulator: self-localized wave packets forming topological edge states residing in the bulk of a nonlinear Floquet photonic topological insulator. Such self-localized wave packets continuously rotate while recreating their shapes periodically, with every cycle of rotation. This kind of a self-trapped wave packet exists by nonlinearly inducing a defect in the bulk of a photonic topological insulator, and populating its own self-induced defect state. The defect then acts as a small domain, and the wave packet rotates around the edge of that domain as an edge state. The induced defect supporting such a wave packet can also operate as an "inner edge" ("hole") in the lattice. In both cases, there is energy flow in the direction dictated by the topological edge state of the underlying structure. Our specific physical system is the same as in Ref. [21]: helical waveguides arranged as a honeycomb lattice. However, the results presented here are universal—applicable to other photonic topological insulator systems [12,28] and to other systems in photonics and beyond, such as exciton-polariton superfluids [29–34], cold atom systems with interactions [35–37], and wherever the underlying physics is described by a Schrödinger-like wave equation.

We begin by describing the underlying linear system. Our system is a two-dimensional waveguide array arranged in a honeycomb lattice. Generally, the array can be described by a tight-binding model (or coupled mode theory) with a discrete set of equations, written as,

$$i\partial_z u_n(z) = \sum_{\langle m\rangle} c_{nm} u_m(z), \tag{1}$$

where the sum is over neighboring sites according to the honeycomb geometry, and the coefficients c_{mn} are the coupling constants between nearest neighbors. Consider the honeycomb lattice of straight waveguides [24], which is the photonic equivalent of graphene. In this case, the coupling coefficients are equal and constant for nearest neighbors: $c_{nm} = c$. In this "ordinary" honeycomb lattice, the first and second bands intersect (without a gap), forming Dirac cones at the corners of the Brillouin zone [24], as is shown in Fig. 1(b). Such a system has trivial topology [21]. To form a Floquet topological insulator, the waveguides can no longer be straight, and take a helical shape with a given longitudinal frequency Ω and radius R [Fig. 1(a)]. In the frame of reference in which the waveguides are stationary, the spinning of the waveguides can be described by introducing a vector potential $\mathbf{A}(z) = A_0[\cos(\Omega z)\hat{x} + \sin(\Omega z)\hat{y}]/a$ to the system [21,38]. Here, a is the lattice constant, and A_0 is a measure of the spinning radius. Thus, the coupling coefficients are modified according to the Peierls' substitution and yield

$$i\partial_z u_n(z) = \sum_{\langle m\rangle} c e^{i\mathbf{A}(z)\cdot\mathbf{r}_{mn}} u_m(z), \tag{2}$$

where $\mathbf{r}_{mn}$ is the displacement between waveguides m and n. Because the right-hand side of Eq. (2) is z dependent, there are no static eigenmodes. Instead, we can define Floquet eigenmodes of the system, based on the fact that in Eq. (2), written as $i\partial_z u_n(z) = \sum_{\langle m\rangle} H_{nm}(z)u_m(z)$, the Hamiltonian $H_{mn}(z)$ is periodic with period $\Lambda = 2\pi/\Omega$ [16,17]. The Floquet eigenmodes are $u_n(z) = e^{i\mu z}\varphi_n(z)$ with $\varphi_n(z)$ being Λ periodic, and μ is the Floquet eigenvalue or "quasienergy." Note that, by definition, the values of μ obey $-\Omega/2 < \mu < \Omega/2$. Thus, we can write $u_n(z+\Lambda) = u_n(z)e^{i\mu\Lambda}$, that is, the wave function $u_n(z)$ self-reproduces every Λ up to a phase. For example, the spectrum for a system with $\Omega = 3c$ and $A_0 = 3$ is shown in Fig. 1(c), and for a system with $\Omega = 6c$ and $A_0 = 2$ in Fig. 1(d). One can clearly see the spectrum in both of these is no longer gapless. The opening of the gap is a consequence of the spinning of the waveguides, which breaks z-reversal symmetry and opens a gap in a mechanism similar to the Haldane model [39]. Inside the gap reside edge states, which are localized states at the edges of finite systems. Because of the topological nature of the system [21,23], these "chiral" edge states have well-defined group velocity and directionality. This means that the edge states are not stationary: they must travel in a given direction, and cannot travel in the opposite direction or stay stationary [21]. In our system, for all parameters of interest, the edge states always rotate clockwise, as schematically shown in Fig. 1(a). These edge states exhibit topological protection: they do not scatter into the bulk nor do they backscatter. This system is exactly a Floquet topological insulator [16,17].

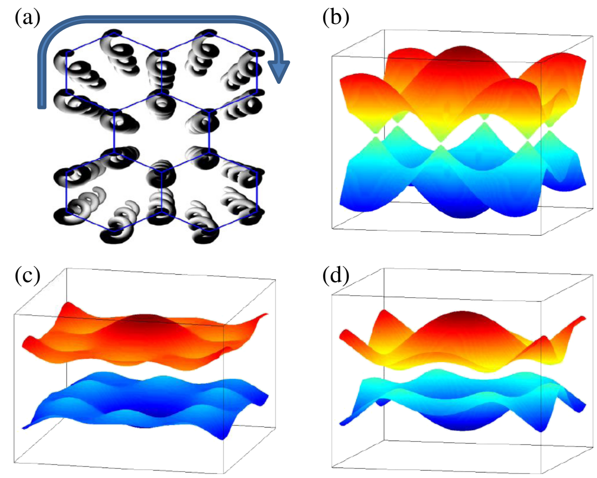

FIG. 1 (color online). (a) Sketch of the honeycomb photonic lattices of spinning waveguides. The rotation axis is in the z direction. The arrow illustrates the propagation direction of topologically protected edge states residing at the edges of the honeycomb lattice. (b) Spatial spectrum (propagation constant vs transverse momentum) of photonic graphene with straight waveguides. (c),(d) Spatial spectra in cases of periodicity $\Omega = 3c$ and radius $A_0 = 3$, and $\Omega = 6c$ and radius $A_0 = 2$, respectively.

Next, we add nonlinearity to the system, and study nonlinear self-localized solutions in the system, i.e., solitons. The nonlinearity we introduce to the system is of the Kerr type, which is also manifested as interactions for cold atom systems. Equation (2) is now transformed into

$$i\partial_z u_n(z) = \sum_{\langle m\rangle} H_{nm}(z)u_m(z) - \sigma|u_n(z)|^2 u_n(z), \tag{3}$$

where $\sigma = \pm 1$ denotes the sign of the nonlinearity, and the strength of it is determined by the magnitude of u_n.

We look for localized solutions in the Floquet sense: wave packets that self-reproduce after a period, but their shape is allowed to vary (and in fact does) within each period. We look for nonlinear solutions using the self-consistency method (commonly used to find solitons in periodic structures [40]), modified to find self-consistent solutions in the Floquet sense. The self-consistency process is described in [41]. We find solitons in the first gap, emerging from the anomalous dispersion (negative effective mass) region in the first band. For such solitons, the nonlinearity is of the defocusing type: $\sigma = -1$ (corresponding to repulsive interactions in cold atom systems). In a similar fashion, one can find fully equivalent gap solitons emerging from the second band under a focusing nonlinearity. In all the examples described in this Letter, we use a system of 338 waveguides (lattice sites), arranged in a parallelogram of 13×13 unit cells. The wave packet is always at the center, well away from the edges of the system. To make sure there are no effects that result from the finite size of the system, we repeated the calculations for different system sizes, and observed no change in the results.

We find self-localized wave packets of different families. We begin by looking for self-localized wave packets that are centered on a site. Consider a concrete example of a honeycomb lattice of helical waveguides under the parameters $A_0 = 3$ and $\Omega = 3c$, for which the gap in the linear system occurs for $-0.44c < \mu < 0.44c$. Naturally, the self-localized wave packets reside in this gap. Figure 2(a) shows the self-localized wave packets' power, defined as $P = \sum_n |u_n|^2$, vs quasienergy. We find that the intensity structure rotates continuously, recreating itself every period. Figures 2(b)–2(d) show the intensity structure of a self-localized wave packet with $P = 4$ and $\mu = 0.08c$, where the intensity is shown every one third of a period. Only the region of the whole lattice where intensity is significant is displayed. Figure 2(e) sketches the rotation of the intensity structure of the wave packet. We determine the direction of rotation also quantitatively, by calculating the energy flow [Fig. 2(f)]. Because the vector potential $\mathbf{A}(z)$ is z dependent, we cannot expect stationary nonlinear solutions (such as bright gap solitons in 2D lattices [42]). In fact, the rotation of the wave packet [Fig. 2(e)] is a direct consequence of the fact that the system is topological in nature. Namely, like edge states of a topological insulator, this nonlinearly self-trapped wave packet rotates in a specific direction. In the case depicted in Fig. 2, we can see that the wave packet inhabits mainly four sites; hence, we can treat the nonlinear change in the potential (induced by the self-localized wave packet) as a four-site defect. This induced defect has edges and edge states. However, because the defect is spatially small, Every point on the defect is on its edge; hence, this wave packet can be interpreted as a self-localized edge state. In fact, recalling the honeycomb geometry and looking at the geometry of the wave packet in Fig. 2(e), we can say that the shape of the self-localized wave packet constitutes the smallest system possible, having well-defined topological edge states [43]. Thus, the self-localized wave packet is a self-induced edge state inside the bulk of the topological insulator, rotating in the direction prescribed by the topological properties of the system. Here, this direction is clockwise, which coincides with the helicity of the lattice. We find that all self-localized states residing on the existence curve of Fig. 2(a) have similar intensity structures and exhibit the same behavior, namely, corotating with the lattice.

We now look for different self-localized wave packets: those that are centered at the center point of a hexagon in the lattice. As an example, consider the lattice with parameters $A_0 = 2$ and $\Omega = 6c$, under which the gap in the linear system is for $-0.32c < \mu < 0.32c$. We find self-localized wave packets residing on the existence curve depicted in Fig. 3(a). A typical intensity structure of such a wave packet is shown in Fig. 3(b) for a self-localized wave packet with $P = 10$ and $\mu = -0.13c$. Only the region of the whole lattice where intensity is significant is displayed. Here, the wave packet occupies mainly six sites, and its intensity structure is approximately constant inside a period. The six sites occupied form the smallest closed

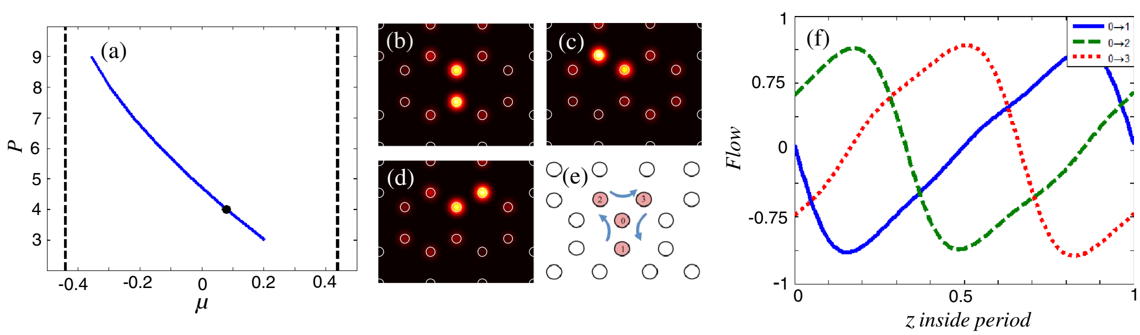

FIG. 2 (color online). (a) Existence curve of power vs quasienergy for solitons with $\Omega = 3c$ and $A_0 = 3$. The black dot is the soliton with $P = 4$. (b),(c),(d) A small region of the lattice, displaying the intensity profile of the soliton with $P = 4$ at $z = 0$, $z = Z/3$, and $z = 2Z/3$, respectively. The white circles denote lattice sites. (e) Schematics of intraperiod power flow. (f) Calculation of power flow between the soliton's main four sites.

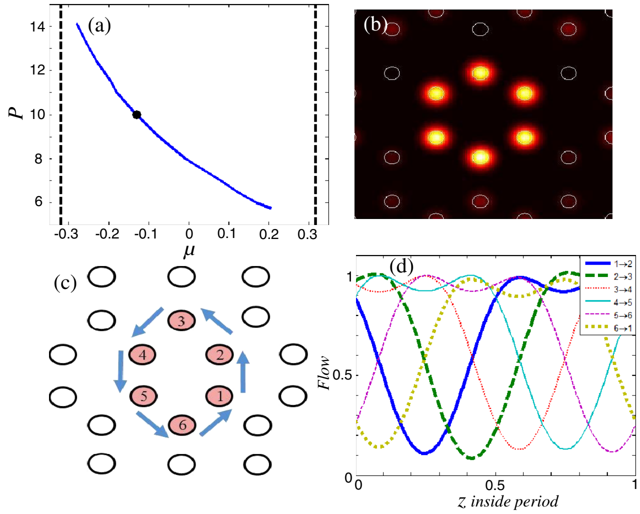

FIG. 3 (color online). (a) Existence curve of power vs quasi-energy for solitons with $\Omega = 6c$ and $A_0 = 2$. The black dot is the soliton with $P = 10$. (b) A small region of the lattice, displaying the intensity of the soliton with $P = 10$. The white circles denote lattice sites. The intensity is approximately constant inside a period. (c) Schematics and (d) calculation of power flow between the soliton's main six sites.

loop possible in the honeycomb geometry. Importantly, despite the constant intensity inside a period, we can still identify the self-localized wave packet as a rotating self-induced edge state. We do so by calculating the power flow between sites inside one period. The energy flow is shown schematically in Fig. 3(c), and quantitatively in Fig. 3(d). We can clearly see a constant, unidirectional power flow in the self-localized wave packet. This flow is significant—the overall flow over a period from one site to the next is about 70% of the average power in these sites. This means that 70% of the total power in the main six sites of the wave packet is flowing around the hexagon over a period. Interestingly, the flow in this case [for all wave packets residing on the existence curve of Fig. 3(a)] is in a counterclockwise direction, opposite to the global edge-state unidirectional flow sketched in Fig. 1(a) and opposite to the spinning direction of the lattice. This can be understood as the induced defect acting as an inner hole, where its edges are inner edges. Basic geometric arguments show that for a system where the outer edge states flow clockwise, the inner edge states should flow counterclockwise, as happens here. One can see that the wave packet in Fig. 3(b) acts as an edge state residing on the edges of an inner hole using the following arguments. The intensity structure of this wave packet forms a closed loop, which constitutes the smallest possible loop in the honeycomb geometry. There is no site inside this loop; hence, the induced defect has a hole in its center. Thus, this induced "defect hole" serves as an inner edge for the bulk. In Fig. 4 we show schematically different inner edges, where it is clear that—when looking at smaller and smaller inner edges—our

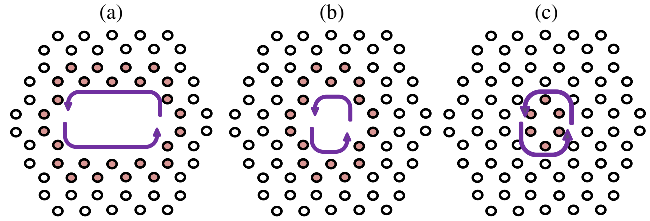

FIG. 4 (color online). (a),(b),(c) Inner edges of a honeycomb lattice of different sizes. (c) A sketch of the soliton presented in Fig. 3.

self-localized wave packet populates the smallest inner edge possible in a honeycomb geometry. An additional geometrical argument for the classification of our wave packet as an inner edge is given in the Supplemental Material [41]. Self-localized wave packets with the same property of being inner holes can also be found with the parameters $A_0 = 2$ and $\Omega = 3c$.

As with all solitons, it is important to examine the stability of our self-localized edge states, which we analyze using both linear stability analysis and numerical simulations. We find that all the self-localized wave packets on the existence curves of Figs. 2(a) and 3(a) are unstable, but the instability can be extremely weak. Quantifying the instability by the number of cycles Λ it takes the wave packet to break up, we find that the instability ranges from tens of cycles to thousands of cycles throughout the existence curve. Thus, despite their instability, these self-localized wave packets can be long-lived and therefore unequivocally observable and of important physical significance.

In conclusion, we presented nonlinear self-localized wave packets in topological insulators. These wave packets are self-induced edge states inside the bulk, and thus rotate with a predetermined directionality. The self-induced edge states can be either outer edges or inner edges, depending on the specifics of the underlying linear system. These nonlinear wave packets are unstable, but long lived, and thus contain much physical significance. Other physical properties would be of great interest—especially the dynamics of multiple such solitons under collisions. Our work lays the groundwork for further study of the effects of nonlinearity in topological insulators in a variety of systems—in optics, exciton-polaritons systems, and cold atoms.

This work was supported by the Israeli Center of Research Excellence (I-CORE) 'Circle of Light', by the Israel Science Foundation, by the Binational USA-Israel Science Foundation (BSF), and by an Advanced Grant from the European Research Council.

[1] C. L. Kane and E. J. Mele, Phys. Rev. Lett. **95**, 226801 (2005).

[2] B. A. Bernevig, T. L. Hughes, and S.-C. Zhang, Science **314**, 1757 (2006).

[3] M. Konig, S. Wiedmann, C. Brune, A. Roth, H. Buhmann, L.W. Molenkamp, X.-L. Qi, and S.-C. Zhang, Science **318**, 766 (2007).
[4] D. Hsieh, D. Qian, L. Wray, Y. Xia, Y.S. Hor, R.J. Cava, and M.Z. Hasan, Nature (London) **452**, 970 (2008).
[5] M.Z. Hasan and C.L. Kane, Rev. Mod. Phys. **82**, 3045 (2010).
[6] K. v. Klitzing, G. Dorda, and M. Pepper, Phys. Rev. Lett. **45**, 494 (1980).
[7] F.D.M. Haldane and S. Raghu, Phys. Rev. Lett. **100**, 013904 (2008).
[8] J. Koch, A.A. Houck, K.L. Hur, and S.M. Girvin, Phys. Rev. A **82**, 043811 (2010).
[9] R.O. Umucalılar and I. Carusotto, Phys. Rev. A **84**, 043804 (2011).
[10] M. Hafezi, E.A. Demler, M.D. Lukin, and J.M. Taylor, Nat. Phys. **7**, 907 (2011).
[11] A.B. Khanikaev, S. Hossein Mousavi, W.-K. Tse, M. Kargarian, A.H. MacDonald, and G. Shvets, Nature Mater. **12**, 233 (2012).
[12] K. Fang, Z. Yu, and S. Fan, Nat. Photonics **6**, 782 (2012).
[13] F. Lederer, G.I. Stegeman, D.N. Christodoulides, G. Assanto, M. Segev, and Y. Silberberg, Phys. Rep. **463**, 1 (2008).
[14] S. Longhi, Laser Photonics Rev. **3**, 243 (2009).
[15] J. Li, R.-L. Chu, J.K. Jain, and S.-Q. Shen, Phys. Rev. Lett. **102**, 136806 (2009).
[16] T. Kitagawa, E. Berg, M. Rudner, and E. Demler, Phys. Rev. B **82**, 235114 (2010).
[17] N.H. Lindner, G. Refael, and V. Galitski, Nat. Phys. **7**, 490 (2011).
[18] Y.T. Katan and D. Podolsky, Phys. Rev. Lett. **110**, 016802 (2013).
[19] Z. Wang, Y.D. Chong, J.D. Joannopoulos, and M. Soljačić, Phys. Rev. Lett. **100**, 013905 (2008).
[20] Z. Wang, Y. Chong, J.D. Joannopoulos, and M. Soljačić, Nature (London) **461**, 772 (2009).
[21] M.C. Rechtsman, J.M. Zeuner, Y. Plotnik, Y. Lumer, D. Podolsky, F. Dreisow, S. Nolte, M. Segev, and A. Szameit, Nature (London) **496**, 196 (2013).
[22] T. Oka and H. Aoki, Phys. Rev. B **79**, 081406(R) (2009).
[23] Z. Gu, H.A. Fertig, D.P. Arovas, and A. Auerbach, Phys. Rev. Lett. **107**, 216601 (2011).
[24] O. Peleg, G. Bartal, B. Freedman, O. Manela, M. Segev, and D.N. Christodoulides, Phys. Rev. Lett. **98**, 103901 (2007).
[25] M. Hafezi, S. Mittal, J. Fan, A. Migdall, and J. Taylor, Nat. Photonics **7**, 1001 (2013).
[26] G.I. Stegeman and M. Segev, Science **286**, 1518 (1999).
[27] G.P. Agrawal, *Nonlinear Fiber Optics* (Academic, San Diego, CA, 1995), 2nd ed; D. Kip, M. Soljacic, M. Segev, E. Eugenieva, and D.N. Christodoulides, Science **290**, 495 (2000).
[28] L. Lu, L. Fu, J.D. Joannopoulos, and M. Soljačić, Nat. Photonics **7**, 294 (2013).
[29] A. Amo, S. Pigeon, D. Sanvitto, V.G. Sala, R. Hivet, I. Carusotto, F. Pisanello, G. Lemenager, R. Houdre, E. Giacobino, C. Ciuti, and A. Bramati, Science **332**, 1167 (2011).
[30] I. Carusotto and C. Ciuti, Rev. Mod. Phys. **85**, 299 (2013).
[31] H. Deng, G. Weihs, C. Santori, J. Bloch, and Y. Yamamoto, Science **298**, 199 (2002).
[32] S. Christopoulos *et al.*, Phys. Rev. Lett. **98**, 126405 (2007).
[33] D. Bajoni, P. Senellart, E. Wertz, I. Sagnes, A. Miard, A. Lemaître, and J. Bloch, Phys. Rev. Lett. **100**, 047401 (2008).
[34] T. Jacqmin *et al.*, arXiv:1310.8105.
[35] L. Tarruell, D. Greif, T. Uehlinger, G. Jotzu, and T. Esslinger, Nature (London) **483**, 302 (2012).
[36] J. Struck, C. Olschlager, R. Le Targat, P. Soltan-Panahi, A. Eckardt, M. Lewenstein, P. Windpassinger, and K. Sengstock, Science **333**, 996 (2011).
[37] I. Bloch and W. Zwerger, Rev. Mod. Phys. **80**, 885 (2008).
[38] A. Crespi, G. Corrielli, G. Della Valle, R. Osellame, and S. Longhi, New J. Phys. **15**, 013012 (2013).
[39] F.D.M. Haldane, Phys. Rev. Lett. **61**, 2015 (1988).
[40] O. Cohen, T. Schwartz, J. Fleischer, M. Segev, and D. Christodoulides, Phys. Rev. Lett. **91**, 113901 (2003).
[41] See Supplemental Material at http://link.aps.org/supplemental/10.1103/PhysRevLett.111.243905 for details of the procedure to compute the wavefunctions and the features of these solitons.
[42] J.W. Fleischer, M. Segev, N.K. Efremidis, and D.N. Christodoulides, Nature (London) **422**, 147 (2003).
[43] Since a wave packet populating a single site cannot exhibit topological protection.